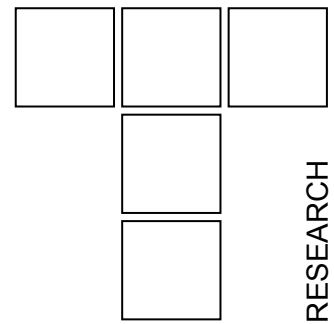


Modeling of Laser-Based Direct Metal Deposition



Central to the success of the metal part fabrication is how well the issues related to process complexity, time, and cost are addressed. Integrating various metal deposition methods in the framework of solid freeform fabrication (SFF) for the varying size and volume of geometrical features along with machining has demonstrated a feasible and economical solution. A number of issues related to laser-based direct metal deposition using the multi-fabrication (MultiFab) system, such as simulation of gas-powder flow, and heat transfer and evolution of residual stresses have been addressed.

Keywords: solid freeform fabrication, laser metal deposition, FEA, CFD

1. INTRODUCTION

To fully realize the potential cost and time savings associated with rapid prototyping (RP) and rapid tooling (RT), the capacity to go from CAD models directly to metal components and tooling is crucial [1]. International competition related to the production of value-added, quality products continues to provide considerable motivation for the development of improved or new manufacturing processes and systems. Solid freeform fabrication (SFF) is one of the fastest growing automated manufacturing technologies that has significantly impacted the length of time between the initial concept and actual part fabrication.

A few of the RP techniques allow the fabrication of fully dense and metallurgically sound metallic parts, suitable for functional testing and application. The techniques such as direct metal deposition (DMD), laser engineered net shaping (LENSTM), and direct light fabrication (DLF) have been used to fabricate the three-dimensional parts of materials such as tool steels, high alloy steels, nickel super alloys, etc.

Srdja Zekovic, Ph.D. candidate, Southern Methodist University, Dallas, Texas, USA, srdjaz@engr.smu.edu
dr Radovan Kovacevic, Herman Brown Chair Professor, Southern Methodist University, Dallas, Texas, USA, kovacevic@engr.smu.edu

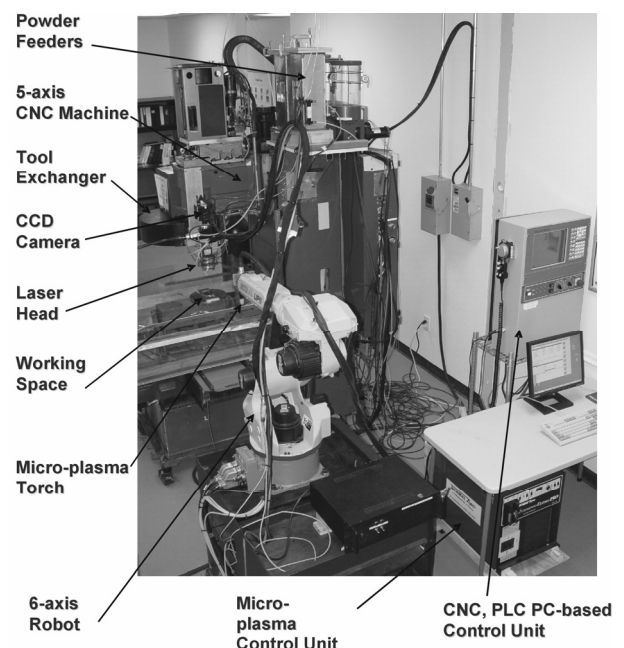


Figure 1. MultiFab system

The multi fabrication (MultiFab) system (Fig. 1.) based on the combination of additive (laser metal deposition and arc welding) and subtractive (milling, drilling and turning) techniques developed at Southern Methodist University is a promising manufacturing system that can be widely applied in solid freeform fabrication (SFF), functionally graded materials (FGM) deposition, component repair and refurbishment, and surface modification [2]. For the SFF application MultiFab system utilizes a 1-kW neodymium-doped yttrium aluminum garnet (Nd:YAG) laser beam in

continuous wave (CW) mode to generate a molten pool onto a metal substrate that concurrently moves along a pre-programmed path. At the same time, the additional material in the form of a metal powder carried by inert gas (Argon) is injected into the molten pool. The solidification of the molten pool after the heat source has passed leaves the additional material fused to the substrate in the form of a bead. Repeating the process on the previously deposited beads as the substrate allows the complex three-dimensional structures to be built directly from the CAD solid model.

The recent achievements on the development of the laser-based direct metal deposition (LBDMD) process at the Research Center for Advanced Manufacturing (RCAM) will be presented in this paper. Special emphasis will be put on the numerical simulation and experimental verification of the gas-powder flow, heat transfer and residual stresses in the LBDMD.

2. NUMERICAL AND EXPERIMENTAL INVESTIGATION OF LASER-BASED DIRECT METAL DEPOSITION (LBDMD) PROCESS

Mathematical modeling could reduce the extent of experimental work required, and thereby to minimize the cost of developing new processes or certifying existing procedures; to provide predictions of operating conditions and the final microstructure and properties for designers, for use on-line, and for failure analysis; and to provide physical insight into the complex mechanisms involved in deposition processes, leading to improved process control. Since the thermal behavior controls the morphology and properties of the specimen, the thermal measurements, microstructure analysis, and modeling can be combined to develop the process parameters to control the microstructure development and to tailor the properties of the specimens to an optimized solution.

To date, the majority of models of thermal-based material processing aimed at developing a deeper understanding of the underlying physics have only concentrated on a specific topic: thermal or mechanical, or microstructure. Little work has addressed the development of a “whole process” model of material processing. A “whole process” model includes thermal, fluid, mechanical, and microstructure sub-models that are coupled together by thermal and chemical histories.

The RCAM research team has been intensively working on the development of the mathematical models for the heat transfer, fluid flow, and thermal stress in the different layered-based and surface treatment processes. RCAM has also developed a two-step numerical model for the LBDMD process.

2.1 Numerical simulation of two phase gas-powder flow

The MultiFab system exploits the multi-axis additive blown-powder laser-based direct metal deposition (LBDMD) process for the near-net fabrication of fully-dense small and intricate features of metallic prototypes by a layered manufacturing method. One of the most important components of a LBDMD is the powder delivery subsystem [3]. It is crucial for the system to deliver powder to the laser-powder interaction zone accurately and repeatedly. The powder delivery subsystem consists of a set of powder feeders, and a radially symmetrical nozzle setup (Fig.2).

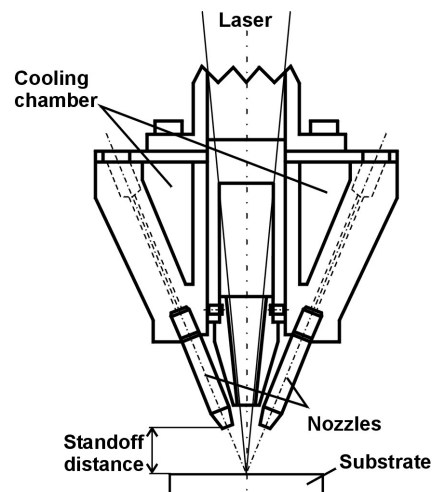


Figure 2. The nozzles setup of the powder delivery system.

To simulate and study powder flow behavior involved in the MultiFab’s powder feeding system, a 3D model of the turbulent gas-powder flow, based on the nozzle setup shown in Fig. 1, has been developed [4]. FLUENT software, based on a finite-volume approach, is used to perform a detailed numerical analysis of the powder stream without laser radiation. Since the gas-powder flow is characterized by the turbulence, and turbulence in turn is a 3D phenomenon, a 3D model is required. The model is used to gain full insight into the process and to analyze the influence of the processing parameters such as the standoff

distance, volumetric gas flow rate, and mass flow rate on the output of the LBDMD process. Also, the developed model provides important parameters for the calculation of the heat transfer boundary conditions for the finite element model (FEM) of the LBDMD process [5].

As it is pointed out, the flow in the nozzles and in the first interaction zone of the laser beam and the metal powder between the nozzles and the substrate is not a simple one-phase turbulent flow. Instead this flow can, at best, be approximated as a two-phase flow, where the primary phase is the inert gas, and the secondary phase consists of the powder particles. The underlying concept is what is usually called the dispersed two-phase flow. The idea is to consider one of the phases (powder particles) to be dispersed in the other one (gas stream) [6]. At the same time, a strong coupling occurs between phases.

The gas-powder mixture injected at the nozzle inlets reaches a fully developed flow while traveling through the nozzles. After the flow leaves the nozzles, the four jets intersect with each other forming a cylindrical area of a maximum powder concentration along the vertical axis in the standoff distance range from -4.75 mm to -6.50 mm (Fig. 3). The powder concentration distribution was approved by projecting sheet of the laser light through the powder cloud and acquiring the digital images of the powder cloud cross sections. Digital images and powder concentration contours are compared in the Fig. 3.

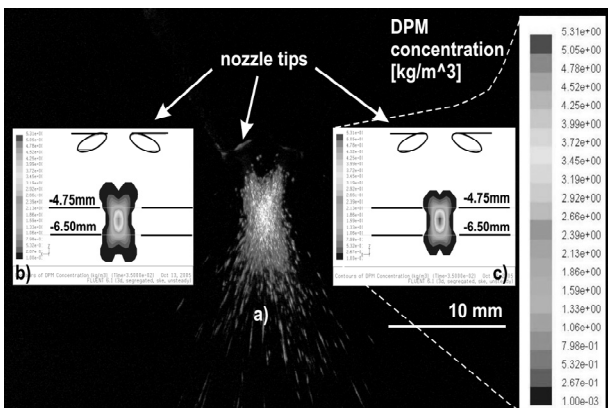


Figure 3. Vertical cross-section of powder cloud below the nozzles: a) digital image, b) concentration contours from simulation in the plane 100 μm offset from the plane of symmetry and c) concentration contours in the plane of symmetry.

2.2 Thermo-structural model for LBDMD

A three-dimensional sequentially coupled thermo-structural FEM model has been developed to perform the heat transfer and residual stress analysis, and to investigate the relationship between the LBDMD processing parameters and the development of residual stress in thin-walled structures. These thin-walled structures are especially subjected to high residual stress as a consequence of the high temperature gradients in the laser metal deposition process and intensive forced convective and the radiative heat transfer from deposited structure to surrounding area.

A sequentially coupled thermal-stress analysis is commonly used in simulations of welding, laser, and e-beam deposition processes since the rather slow stress development affects heat transfer very little. Such an analysis is not only fast and computationally economical, but also allows for all useful features of individual thermal and stress analyses available in FEA packages to be applied. Three-dimensional transient thermal analysis is conducted first to obtain the global temperature history generated during the laser deposition process. A transient stress analysis is then developed with temperatures obtained from thermal analysis entered as loading to the stress model.

2.2.1 Heat flow analysis

Since LBDMD is a thermal process, the well-known heat conduction plays a central role in the physical modeling of the process. The governing energy balance for conduction-dominated heat flow with a moving heat source in an elementary volume is:

$$\rho c \frac{\partial T}{\partial t} = \mathcal{Q} + k \left[\frac{\partial^2 T}{\partial x^2} + \frac{\partial^2 T}{\partial y^2} + \frac{\partial^2 T}{\partial z^2} \right] + \frac{\partial k}{\partial T} \left[\left(\frac{\partial T}{\partial x} \right)^2 + \left(\frac{\partial T}{\partial y} \right)^2 + \left(\frac{\partial T}{\partial z} \right)^2 \right] \quad (1)$$

where, (x, y, z) are coordinates in the domain D , t is time, $T(x, y, z, t)$ is temperature, $\rho = \rho(T)$ is the density, $c = c(T)$ is heat capacity, $k = k(T)$ is heat conductivity, and $\mathcal{Q}(x, y, z, t)$ is volumetric heat generation.

Beside the dominant influence of the heat conduction, the heat losses by forced convection and radiation are included in thermal analysis, and they are incorporated in the model as boundary conditions for specific areas of the structure such as those areas closer or farther from the molten pool. Since an incorporation of the radiation effects

are found to increase the solution by as much as three times, an approximation can be made using only the convective term,

$$k_n \frac{\partial T}{\partial n} = h_e (T - T_a) \quad (2)$$

with an equivalent heat transfer coefficient h_e that combines the effects of radiation and convection, and where h_e is defined by an empirical relationship as proposed by Goldak [7].

Laser metal deposition takes place under the intensive flow of inert gas argon from radially symmetrical four nozzles. Consequently, the forced convection heat transfer on the wall and substrate surfaces must be considered using the appropriate boundary condition:

$$k_n \frac{\partial T}{\partial n} = h_f (T - T_a) \quad (3)$$

where $h_f = f(v, z)$ is the coefficient of the forced convection for the flat plate as a function of gas velocity v , and wall height z [8].

Because of the wide temperature range in the deposited structure, the thermal material properties are clearly nonlinear; that is, the heat capacity and thermal conductivity are temperature-dependent. As the effects of the latent heat accompany the properties, the phase changes of the material, both solid-solid and solid-liquid, are of the particular interest. The latent heat changes during martensitic transformation and solidification take place over finite temperature intervals and can be presented by equivalent temperature distribution of enthalpy H . Knowing the values of the latent heat of fusion and transformation, the latent heat effects of the phase changes can be incorporated in the form of an equivalent increase of the heat capacity. Consequently, some numerical instability in the FEA software that was used in this work can be avoided.

2.2.2 Thermal stress analysis

In sequentially coupled analysis, the mechanical fields are analyzed, proceeding from already known, temperature fields that are considered as the only load. The total strain $d\varepsilon_{ij}$ is composed of elastic strain $d\varepsilon_{eij}$, conventional plastic strain $d\varepsilon_{pij}$, plastic strain from transformation plasticity $d\varepsilon_{tpij}$, and thermal strain $d\varepsilon_{Tij}$:

$$d\varepsilon_{ij} = d\varepsilon_{eij} + d\varepsilon_{pij} + d\varepsilon_{tpij} + d\varepsilon_{Tij} \quad (4) \quad (i, j = 1, 2, 3)$$

For residual stress analysis, in addition to density ρ , the following thermo-mechanical material properties depending on temperature are required: thermal expansion coefficient α , elastic modulus E , Poisson's ratio ν , and yield strength σ_Y . However, the values for the higher range of temperatures and phase transformations are based on the experimental results, relationships, and extrapolation schemes suggested by several authors [7,9-10]. In the thermo-mechanical material model, the transformation-induced plasticity is incorporated by the reduction of yield strength, while an equivalent change of the thermal expansion introduces the volume change during the phase transformation. The adequacy of these assumptions is, of course, open to question, and only the experimental determination of the required high temperature data can serve to test its validity.

2.2.3 Finite element model

The general purpose FE package ANSYS is used for both the thermal and the stress analyses performed sequentially with an appropriate combination of elements. The algorithm for a residual-stress analysis is summarized in Fig. 4. The main features of the 3D model are the moving heat input, element birth-and-death technique, heat loss, temperature-dependent material properties, and application of ANSYS parametric design language (APDL) to the model moving heat source, and adaptive boundary conditions [11].

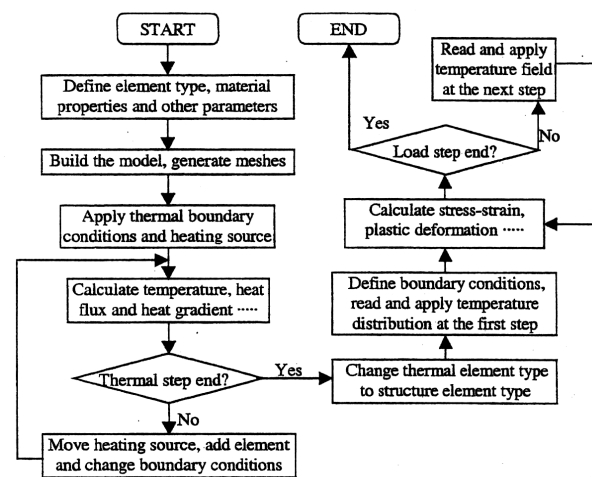


Figure 4. Algorithm of thermo-structural analysis

The powder and gas velocity distribution obtained from the model of the gas-powder flow (Fig. 5) have been used to calculate adaptive boundary

conditions for the thermal analysis during the deposition.

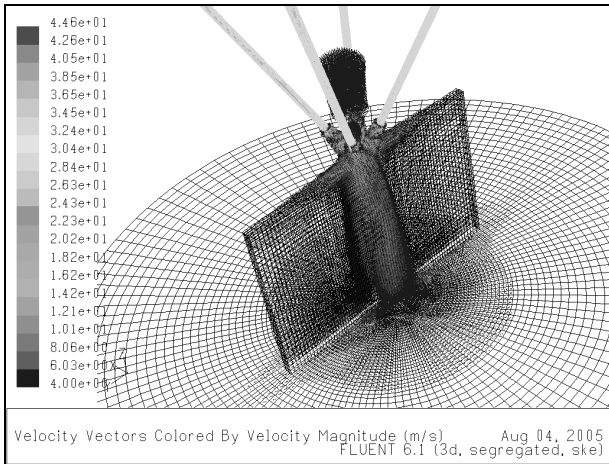


Figure 5. Velocity vectors of the gas flow around thin wall

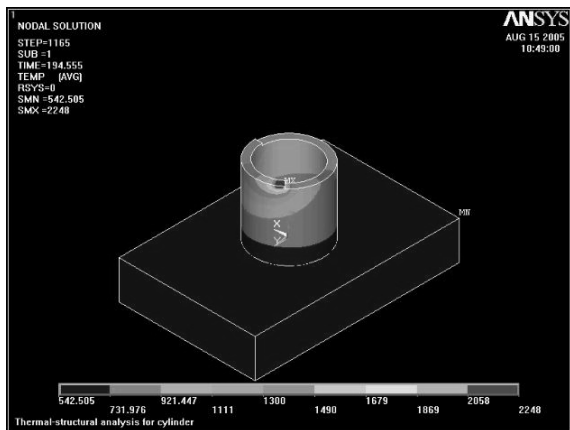
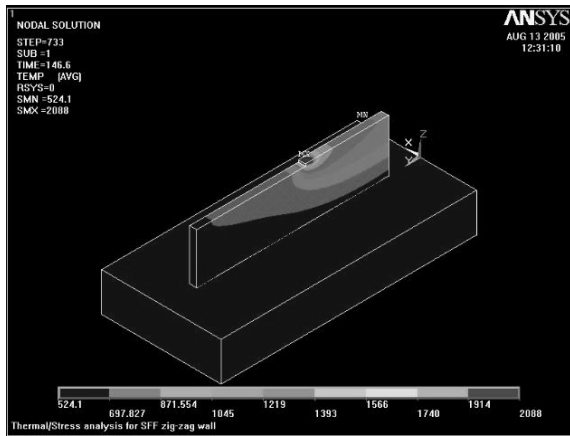


Figure 6. Temperature during deposition: a) zig-zag deposited straight wall, b) cylinder

Three cases are studied: a straight wall fabricated by the zig-zag deposition strategy, a straight wall fabricated by the one-direction deposition strategy,

and a cylindrical wall fabricated by the one-direction deposition strategy.

The model makes it possible to analyze the influence of the deposition strategy and part geometry on temperature distribution (Fig. 6) and residual stress development (Fig. 7). The residual stress distribution gives an explanation for some of the phenomena observed during the deposition process.

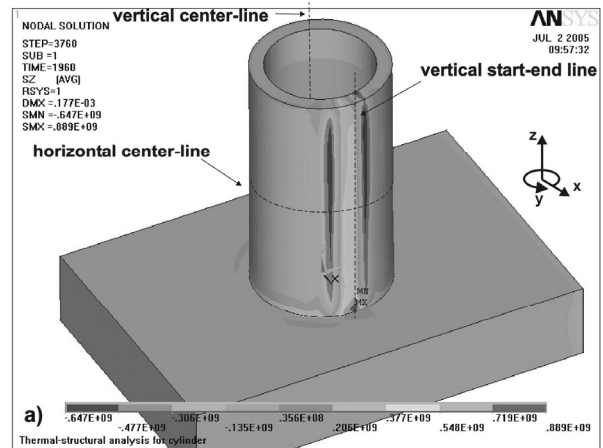
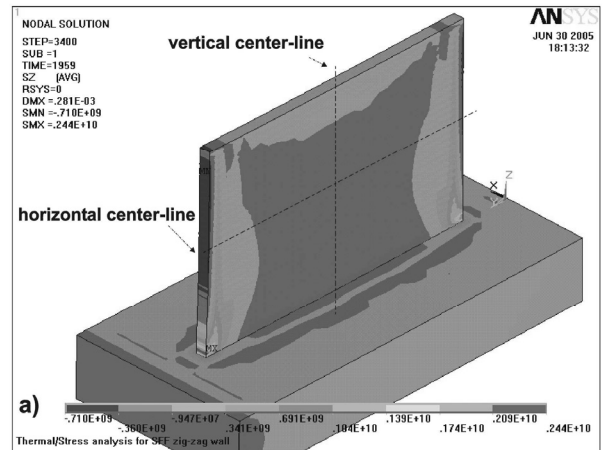


Figure 7. Residual stress in: a) zig-zag deposited straight wall and b) cylinder

The material used in this investigation was an H13 tool steel that is the material of choice for the die and tool industry. As the most uniform temperature distribution is observed in the cylindrical wall, it causes the lowest residual stress, far below the tensile strength of the material and a stable deposited structure (Fig. 8a). On the other side, the stress level at the corners of the zig-zag deposited straight wall is above tensile strength, which causes a cracked appearance (Fig. 8b).

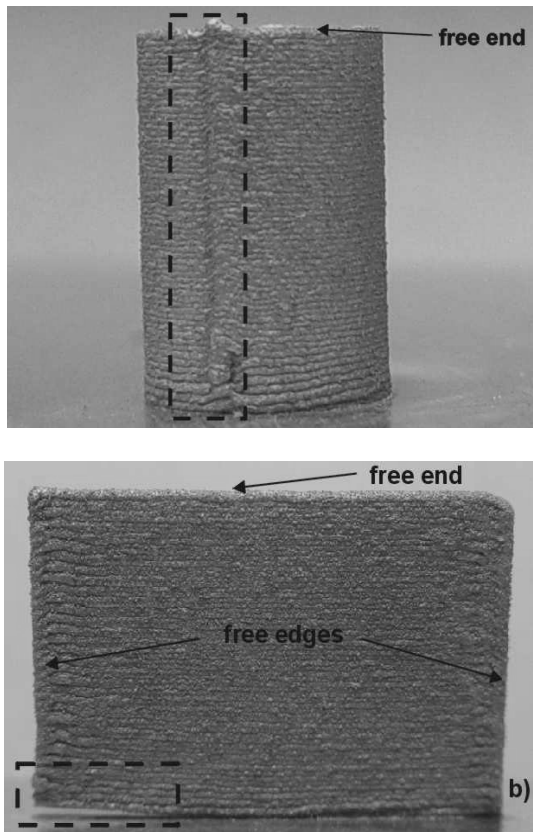


Figure 8. Deposited structures: a) cylinder and b) straight wall

Furthermore, the zig-zag deposition strategy induces shear stress between subsequent layers in a straight wall buildup. The predicted temperature history by the FEA has been verified experimentally by employing the thermocouples [5]. A qualitative comparison of the residual stress pattern show a good agreement between the FE model and experimental results obtained by neutron diffraction of a straight thin-walled structures built in a similar experiment [12].

The analysis results provide a better understanding of the LBDMD process and give directions for the optimization of the processing parameters like heat input, material input, as well as the deposition strategy with the final goal - improved strength and service life of a fabricated structure.

3. CONCLUSIONS

A set of issues related to the laser-based direct metal deposition applied using the framework of SFF were identified and discussed. The optimization of the process, that includes metal powder delivery, heat transfer, and stress evolution is done and suitable parameters are identified. A set of experiments confirm the effectiveness of the

suggested parameters and the process planning methods.

REFERENCES

- [1] Beaman, J.J., J. W. Barlow, R. H. Bourell, H. L. Craford, H. L. Marcus and K. P. McAlea, Solid Freeform Fabrication: A New Development in Manufacturing, Kluwer Academic Publishers, Dordrecht / Boston / London, 1997.
- [2] Kovacevic, R., Valant, M., System and Method for Fabrication or Repairing Part, US Patent No. 7,020,539, Issued on March 28, 2006.
- [3] Valant, M., Kovacevic, R., Powder Delivery System, US Patent No. 7,045,738 issued on May 16, 2006.
- [4] Zekovic S., Dwivedi R., Kovacevic R., Numerical simulation and experimental investigation of gas-powder flow from radially symmetric nozzles in laser-based direct metal deposition, International Journal of Machine Tools & Manufacture, Design, Research and Application, (accepted for publication, February 2006).
- [5] Zekovic, S., Dwivedi, R., Kovacevic, R., Thermo-structural Finite Element Analysis of Direct Laser Metal Deposited Thin-Walled Structures, Proceedings SFF Symposium, Austin, TX, August 2005.
- [6] Fluent Inc., FLUENT 6.2.1 User Guide, 2004.
- [7] Goldak, J., Chakravarti, A., Bibby M., A New Finite Element Model for Welding Heat Sources, Metallurgical Transactions B, Vol.15B, June 1984, pp.299-305.
- [8] Holman J.P., Heat transfer, 7th edition, McGraw Hill Book Company, New York, 1990.
- [9] Radaj, D., Heat Effects of Welding; Temperature Field, Residual Stresses, Distortion, Springer-Verlag, New York, 1992.
- [10] Ready, J.F., LIA Handbook of Laser Materials Processing, 1st edition, Laser Institute of America, Orlando, 2001, ISBN 0-912035-15-3.
- [11] ANSYS Inc., "ANSYS Theory Manual, Release 8.1," USA, 2004.
- [12] Rangaswamy, P., Holden, T.M., Rogge, R.B. and Griffith, M.L., Residual Stresses in Components Formed by the Laser-Engineered Net Shaping (LENSTM) Process, The Journal of strain analysis for engineering design, Vol.38, No.6, November 2003, pp. 519-527